Effect of the type-I to type-II Weyl semimetal topological transition on superconductivity

Dingping Li,[1,2,*] Baruch Rosenstein,[3,†] B. Ya. Shapiro,[4,‡] and I. Shapiro[4]
[1]*School of Physics, Peking University, Beijing 100871,* China
[2]*Collaborative Innovation Center of Quantum Matter, Beijing, China*
[3]*Electrophysics Department, National Chiao Tung University, Hsinchu 30050,* Taiwan, Republic of China
[4]*Physics Department, Bar-Ilan University, 52900 Ramat-Gan, Israel*
(Received 28 December 2016; revised manuscript received 27 January 2017; published 21 March 2017)

The influence of recently discovered topological transition between type-I and type-II Weyl semimetals on superconductivity is considered. A set of Gorkov equations for weak superconductivity in Weyl semimetal under topological phase transition is derived and solved. The critical temperature and superconducting gap both have spikes in the transition point as functions of the tilt parameter of the Dirac cone determined, in turn, by the material parameters like pressure. The spectrum of superconducting excitations is different in two phases: The sharp cone pinnacle is characteristic for type I, while two parallel almost flat bands, are formed in type II. Spectral density is calculated on both sides of transition to demonstrate the different weights of the bands. The superconductivity thus can be used as a clear indicator for the topological transformation. Results are discussed in the light of recent experiments.

DOI: 10.1103/PhysRevB.95.094513

I. INTRODUCTION

The effect of the Fermi surface topology on properties of a crystalline conductor was a subject of theoretical investigations over the years [1]. Experimentally, a continuous deformation of the Fermi surface (without changing the chemical nature of the crystal) can be experimentally achieved by external factors like pressure and electric field. Historically, transitions associated with a change of topology were called "2.5 transition" [2]. Transport in materials with low electron density is especially sensitive to modification of the Fermi surface [3], while these transitions were predicted to make a great impact on the superconducting state [4]. Recently, a new class of such materials made the phenomenon important in a very different setting. A broad number of low-electron-density two-dimensional (2D) and 3D Weyl semimetals were discovered. Most of them are characterized by linear dispersion relation near the Fermi surface. Topology and even dimensionality of the small Fermi surface in these materials are linked to the Berry phases of their band structure [5]. The first material of this class, graphene [6], exhibits the highest symmetry leading to a linear ultrarelativistic spectrum; however, most of the other materials are anisotropic. Examples include 2D Weyl semimetals (WSMs) silicene, germanene, and borophene [7] and 3D crystals [8] Na_3Bi and [9] Cd_3As_2 and numerous layered organic compounds [10–12]. Topological insulators (TIs) like Bi_2Se_3 and others [13] generally have Dirac cones on their surfaces of topological insulators.

It was realized recently that this variety of novel materials should be differentiated between the more isotropic "type-I" Weyl semimetals [14,15] [see Fig. 1(a)] and highly anisotropic type-II Weyl semimetals in which the cone of the linear dispersion relation is tilted beyond a critical angle [Fig. 1(b)]. The newer type-II Weyl fermion materials, WTe_2, exhibit exotic phenomena such as angle-dependent chiral anomaly [14]. The discovery of a Weyl semimetal in TaAs offers the first Weyl fermion observed in nature and dramatically broadens the classification of topological phases. Other dichalkogenides like [16] $MoTe_2$ and [17] $PtTe_2$ were demonstrated to be type-II Weyl semimetals. In particular, the series $Mo_xW_{1-x}Te_2$ inversion-breaking, layered, tunable semimetals is already under study as a promising platform for new electronics and recently proposed to host type-II Weyl fermions [18] . Some other materials, like layered organic compound $\alpha - (BEDT - TTF)_2I_3$, were long suspected [11] to be a 2D type-II Dirac fermions. Several classes of materials were predicted via band structure calculations to undergo the I-to-II transition while doping or pressure is changed [19].

Theoretically, physics of the transitions between the type-I and type-II Weyl semimetals were considered in the context of superfluid phase [5] A of He_3, layered organic materials in 2D [12] and 3D Weyl semimetals [20]. The pressure modifies the spin-orbit coupling that, in turn, determines the topology of the Fermi surface of these novel materials [15]. Very recently the topological transition in Weyl semimetal under pressure was observed [21].

This transition is an ideal example of the 2.5 transition mentioned above. Both the Fermi surface reconstruction and low electron density are present in the extreme in these materials. It is generally difficult to find good indicators for such a transition. Since superconductivity is especially affected by the 2.5 transition it might serve as the indicator. Indeed, some Weyl materials are known to be superconducting. The surface of the well-known TI Bi_2Se_3 exhibits under certain conditions superconductivity of up to [22] 8 K; some organic materials like [23] $\kappa - (BEDT - TTF)_2X$, with $X = I_3$, or other anion [24] are superconducting.

A detailed study of superconductivity in TIs under hydrostatic pressure revealed a curious dependence of critical temperature of the superconducting transition on pressure [25].

*Corresponding author: lidp@pku.edu.cn
†vortexbar@yahoo.com
‡shapib@mail.biu.ac.il

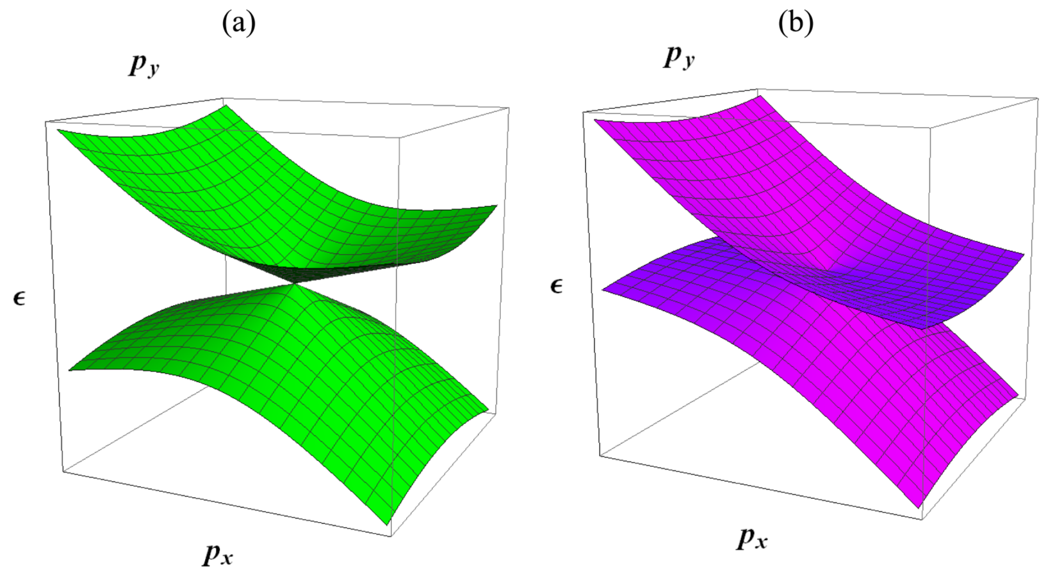

FIG. 1. Spectrum of normal Weyl semimetal. (a) Type I ($w/v = 0.5$). (b) Strongly tilted Dirac cone for the type-II semimetals ($w/v = 1.2$).

In intercalated $Sr_{0.065}Bi_2Se_3$, a single crystal [26] considered to be a pure material, ambient weak superconductivity first is suppressed, but at a high pressure of 6 GPa it reappears and reaches a relatively high T_c of 10 K that persists up to 80 GPa. The increase is not gradual, but rather abrupt in the region of 15 GPa [26]. Superconductivity in similar TI compounds [27–29] Bi_2Se_3, Bi_2Te_3, and 3D Weyl semimetal [30] $HfTe_5$ was also studied experimentally. The critical temperature T_c in some of these systems shows a sharp maximum as a function of pressure. This contrasts with generally smooth dependence on pressure in other superconductors (not suspected to be Weyl materials), like a high-T_c cuprate [31] YBCO. Various mechanisms of superconductivity in Dirac semimetals and topological insulators turned superconductors have been considered theoretically [32–34]. A theory predicting the possibility of superconductivity in the type-II Weyl semimetals was developed recently in the framework of the Eliashberg model [35].

We show in this paper that superconducting critical temperature and energy gap features are efficient markers of the topological type-I-to-type-II transition under pressure. The s-wave pairing in a general Weyl semimetal with tilted Dirac cones is considered in the framework of the boson-mediated adiabatic regime. We calculate the critical temperature T_c and the energy gap Δ at zero temperature for arbitrary tilt (controlled by pressure in certain materials) and find their sharp increase at the topological transition point from type-I to type-II Weyl semimetal.

II. TYPE-I AND TYPE-II WEYL SEMIMETAL WITH LOCAL PAIRING INTERACTION

Weyl material typically possesses several sublattices. We exemplify the effect of the topological transition on superconductivity using the simplest possible model with just two sublattices denoted by $\alpha = 1,2$. The band structure near the Fermi level of a 2D Weyl semimetal is well captured by the following Hamiltonian:

$$K = \int_{\mathbf{r}} \psi_\alpha^{sL+}(\mathbf{r}) K_{\alpha\beta}^L \psi_\beta^{sL}(\mathbf{r}) + \psi_\alpha^{sR+}(\mathbf{r}) K_{\alpha\beta}^R \psi_\beta^{sR}(\mathbf{r}),$$
$$K_{\alpha\beta}^{L,R} = -i\hbar v\left(\nabla_x \sigma_{\alpha\beta}^x \mp \nabla_y \sigma_{\alpha\beta}^y\right) + (-i\hbar \mathbf{w}\cdot\nabla - \mu)\delta_{\gamma\delta}. \quad (1)$$

Here v is Fermi velocity, μ is the chemical potential, σ are Pauli matrices in the sublattice space, and s is the spin projection. Generally, there are a number of pairs of points (Dirac cones) constituting the Fermi "surface" of such a material at chemical potential $\mu = 0$. We restrict ourself to the case of just one left-handed (L) and one right-handed (R) Dirac points, typically but not always separated in the Brillouin zone. Generalization to several pairs is straightforward. The 2D velocity vector $\mathbf{w}$ defines the tilt of the cone; see the dispersion relation of one of the cones in Fig. 1. The graphenelike dispersion relation in Fig. 1(a) for $w = 0.5$ represents the type-I Weyl semimetal, while when the length of the tilt vector exceeds v [Fig. 1(b)], the material becomes a type-II Weyl semimetal.

The effective electron-electron attraction due to either electron-phonon attraction and Coulomb repulsion (pseudopotential) or some unconventional pairing mechanism creates pairing. We assume that different valleys are paired independently and drop the valley indices (multiplying the density of states by $2N_f$). Further, we assume the local singlet s-channel interaction Hamiltonian,

$$V = \frac{g^2}{2}\int d\mathbf{r}\ \psi_\alpha^{+\uparrow}(\mathbf{r})\psi_\beta^{\downarrow+}(\mathbf{r})\psi_\beta^{\uparrow}(\mathbf{r})\psi_\alpha^{\downarrow}(\mathbf{r}). \quad (2)$$

As usual, the interaction has a cutoff frequency Ω, so that it is active in an energy shell of width $2\hbar\Omega$ around the Fermi level [36]. For the phonon mechanism it is the Debye frequency.

III. SPECTRUM OF EXCITATIONS IN THE SUPERCONDUCTING STATE

Finite-temperature properties of the condensate are described by the normal and the anomalous Matsubara

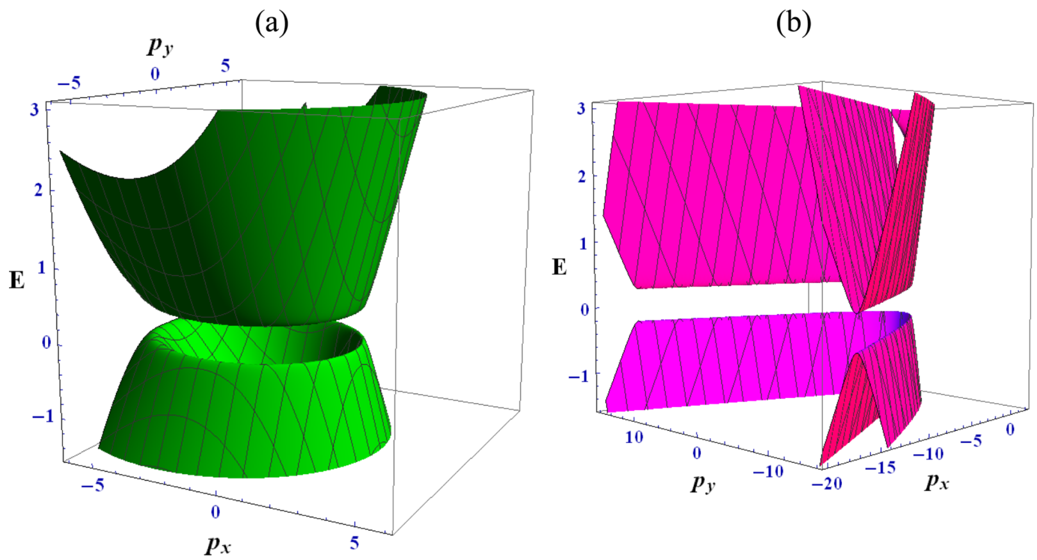

FIG. 2. Spectrum of superconducting quasiparticles as function of momentum (in units of $\hbar\Omega/v$) for (a) type-I ($w/v = 0.5$) and (b) type-II ($w/v = 1.2$) Weyl semimetal for chemical potential $\mu = 3$ and energy gap $\Delta = 0.25$ (in units of phonon energy $\hbar\Omega$).

Green's functions [36],

$$G^{ts}_{\alpha\beta}(\mathbf{r}\tau,\mathbf{r}'\tau') = -\langle T_\tau \psi^t_\alpha(\mathbf{r}\tau)\psi^{s+}_\beta(\mathbf{r}'\tau')\rangle = \delta^{ts} g_{\alpha\beta}(\mathbf{r}-\mathbf{r}',\tau-\tau'),$$
$$F^{ts}_{\alpha\beta}(\mathbf{r}\tau,\mathbf{r}'\tau') = \langle T_\tau \psi^t_\alpha(\mathbf{r}\tau)\psi^{s}_\beta(\mathbf{r}'\tau')\rangle = -\varepsilon^{ts} f_{\alpha\beta}(\mathbf{r}-\mathbf{r}',\tau-\tau'),$$
$$F^{+ts}_{\alpha\beta}(\mathbf{r}\tau,\mathbf{r}'\tau') = \langle T_\tau \psi^{t+}_\alpha(\mathbf{r}\tau)\psi^{s+}_\beta(\mathbf{r}'\tau')\rangle = \varepsilon^{ts} f^{+}_{\alpha\beta}(\mathbf{r}-\mathbf{r}',\tau-\tau'). \quad (3)$$

The second equality in each line relies on homogeneity and unbroken invariance under spin rotations. The gap function in the s-wave channel is

$$\Delta_{\alpha\gamma} \equiv -\frac{g^2}{4}\varepsilon^{s_3 s_2}\langle \psi^{s_3}_\alpha(\mathbf{r},\tau)\psi^{s_2}_\gamma(\mathbf{r},\tau)\rangle = \sigma^x_{\alpha\gamma}\Delta. \quad (4)$$

In terms of Fourier transforms, $g_{\gamma\kappa}(r,\tau) = T\sum_{\omega\mathbf{p}} \exp[i(-\omega\tau + \mathbf{p}\cdot\mathbf{r})]g_{\gamma\kappa}(\omega,p)$, the Gorkov equations read (see Appendix A)

$$[v\mathbf{p}\cdot\sigma_{\gamma\beta} + (i\omega + \mu - wp_x)\delta_{\gamma\beta}]g_{\beta\kappa}(\omega,p) + \Delta\sigma^x_{\alpha\gamma} f^+_{\alpha\kappa}(\omega,p) = \delta^{\gamma\kappa},$$
$$[v\mathbf{p}\cdot\sigma_{\beta\gamma} + (-i\omega + \mu - wp_x)\delta_{\gamma\beta}]f^+_{\beta\kappa}(\omega,p) - \Delta^*\sigma^x_{\gamma\alpha} g_{\alpha\kappa}(\omega,p) = 0. \quad (5)$$

The Matsubara frequency at temperature T takes values $\omega_n = \pi T(2n+1)$, and units are chosen such that $\hbar = 1$. We have chosen coordinates in such a way that the vector w causing the tilt of the Dirac cone is oriented along the x axis. In matrix form (in sublattice space) we obtain the solution (see Appendix A)

$$\widehat{g}(\omega,\mathbf{p}) = \sigma^x[\mathbf{p}\cdot\sigma^t + (-i\omega + \mu - wp_x)I]M^{-1},$$
$$\widehat{f}^+(\omega,\mathbf{p}) = M^{-1}\Delta^*, \quad (6)$$

where

$$M = [v\mathbf{p}\cdot\sigma + (i\omega + \mu - wp_x)I] \times \sigma^x[v\mathbf{p}\cdot\sigma^t + (-i\omega + \mu - wp_x)I] + |\Delta|^2\sigma^x, \quad (7)$$

and I is the identity matrix. The determinant of M,

$$\det M = -[\Delta^2 + \omega^2 + (vp - \mu + wp_x)^2] \times [\Delta^2 + \omega^2 + (-vp - \mu + wp_x)^2], \quad (8)$$

continued to physical energy, $\omega \to -iE$, gives the spectrum of quasiparticles

$$E^2_\pm = \Delta^2 + (\pm vp - \mu + wp_x)^2, \quad (9)$$

depicted for type-I and type-II Weyl semimetals in Fig. 2.

The quasiparticle spectrum is very different. In a superconducting graphenelike material for $\mu \gg \Delta$, the energy gap is minimal on the circle of radius μ/v; see Fig. 2(a). Note that the sharp cone pinnacle in the excitations spectrum wedge is formed at the former cone location. For the type-II Weyl semimetal turned superconductor [Fig. 2(b)] the low-energy spectrum consists of two parallel flat bands, while the pinnacle disappears.

Spectral density

The spectral density function,

$$A(E,\mathbf{p}) = -\frac{1}{\pi}\mathrm{ImTr}\,\widehat{g}(-iE + \eta,\mathbf{p}),$$
$$\mathrm{Tr}\,\widehat{g}(\omega,\mathbf{p}) = \frac{2}{\det M}\{[v^2p^2 - (\mu - wp_x - i\omega)^2] \times (\mu - wp_x + i\omega) - \Delta^2(\mu - wp_x - i\omega)\}, \quad (10)$$

presented in Fig. 3, where different weights of the dispersion law branches accompanied type-I-to-type-II transition. Here η is the "disorder" parameter; $\widehat{g}(\omega,\mathbf{p})$ is defined by Eq. (6).

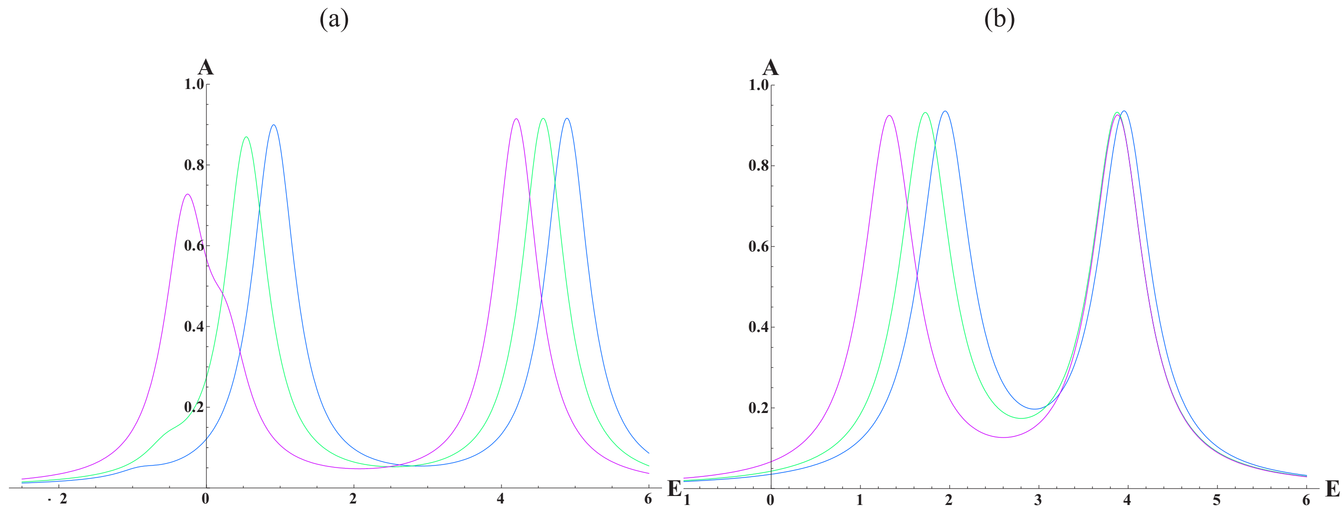

FIG. 3. Spectral density $A(\mathbf{p},E)$ for type-I (a) $(w/v = 0.5)$ and type-II (b) $(w/v = 1.2)$ superconducting semimetals. Here $p_x = 1,\ p_y = 0.1$ (green), 0.4 (red), 0.8 (blue) in units of $\hbar\Omega/v$. Here $\mu = 3,\ \Delta = 0.25$ (in the units of cut off phonon energy $\hbar\Omega$).

IV. CRITICAL TEMPERATURE AND THE ENERGY GAP

The gap as a function of the material parameters is determined by the equation

$$\Delta^* = \frac{\Delta^*}{2(2\pi)^3} T \sum_{\omega} \int d\mathbf{p}\ \mathrm{Tr}[\sigma_x M^{-1}], \tag{11}$$

resulting in, at zero temperature,

$$\frac{1}{g^2} = \frac{1}{(2\pi)^3} \int d\omega d\mathbf{p} \frac{v^2 p^2 + \Delta^2 + (\mu - w p_x)^2 + \omega^2}{[\Delta^2 + (vp + wp_x - \mu)^2 + \omega^2][\Delta^2 + (vp - wp_x + \mu)^2 + \omega^2]}. \tag{12}$$

Performing integration on ω and momenta subject to restriction of being inside the energy shell of Ω around the Fermi level; see Fig. 4, one obtains in the adiabatic limit $\mu \gg \Omega \gg \Delta$, after integration over azimuthal angle (see Appendix B for details),

$$\frac{1}{g^2} = \frac{\mu}{4\pi v^2} f(\kappa) \ln\left[\frac{2\Omega}{\Delta}\right]. \tag{13}$$

Here $\kappa = w/v$ is the anisotropy parameter. The function f is

$$f(\kappa) = \begin{cases} \frac{2}{(1-\kappa^2)^{3/2}} & \text{for } \kappa < 1, \\ \frac{2\kappa^2}{\pi(\kappa^2-1)^{3/2}}\left\{2\sqrt{1+\kappa} - 1 + \ln\frac{2(\kappa^2-1)}{\kappa(1+\sqrt{1+\kappa})^2\delta}\right\} & \text{for } \kappa > 1, \end{cases} \tag{14}$$

where $\delta = \pi a\Omega/v\hbar$ is the cutoff parameter and a is the interatomic distance. [The effective density of states $f(\kappa)$ formally diverges at $\kappa = 1$. It is the result of linear dispersion relation in the model Weyl Hamiltonian. Indeed, the linear approximation of the dispersion relation in the Weyl semimetal is valid only for the small neighborhood of the Dirac point. At higher energies the band spectrum is nonlinear and cut off by the bandwidth $1/a$. Actual cutoff is not very important since the singularity is logarithmic.]

The superconducting gap in this case therefore is (returning to physical units)

$$\Delta = 2\hbar\Omega \exp\left[-\frac{1}{\lambda f(\kappa)}\right], \tag{15}$$

where $\lambda = N(\mu)g^2$ is the conventional effective electron-electron dimensionless coupling constant and $\ln[\gamma_E] = 0.577$. Dependence is presented in Fig. 5. The effective density of states (DOS) $D(E,\kappa) = N(E \to \mu) f(\kappa)$ in the normal state for N_f pairs of Dirac cones is $\frac{2N_f}{4\pi v^2}\mu f(\kappa)$. This DOS coincides with the spectral density given in Eq. (10) for $\Delta = 0$ integrated over momenta, $D(E,\kappa) = \int d\mathbf{p}\ A(E,\mathbf{p},\kappa)$.

The critical temperature is defined from the gap equation, when the gap Δ vanishes:

$$\frac{1}{g^2} = \frac{T}{(2\pi)^2} \int d\mathbf{p} \sum\nolimits_n \times \frac{v^2 p^2 + (\mu - wp_x)^2 + \omega_n^2}{[(vp + wp_x - \mu)^2 + \omega_n^2][(vp - wp_x + \mu)^2 + \omega_n^2]}. \tag{16}$$

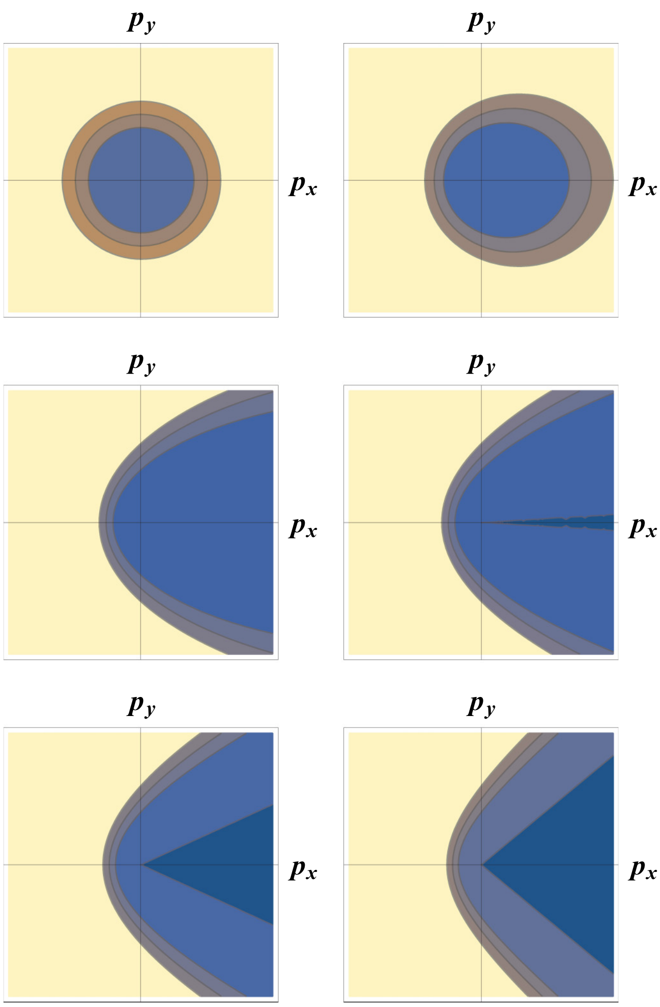

FIG. 4. Equipotential surfaces of the electron energy for different ratio w/v (pairs of the figures from top to bottom): top row, $w/v = 0.01$ (left), $w/v = 0.4$; middle row, $w/v = 0.91$ (left), $w/v = 1.004$; and bottom row, $w/v = 1.1$ (left), $w/v = 1.4$.

The sum over Matsubara frequencies can be done,

$$\frac{1}{g^2} = \frac{1}{4(2\pi)^2}\int d\mathbf{p}\left\{\frac{\tanh\left[|vp + wp_x - \mu|/2T\right]}{|vp + wp_x - \mu|} + \frac{\tanh\left[|vp + wp_x + \mu|/2T\right]}{|vp + wp_x + \mu|}\right\}. \quad (17)$$

In the adiabatic approximation, $\mu \gg \Omega$, performing integration one obtains

$$\frac{1}{g^2} \approx \frac{\mu f(\kappa)}{4\pi v^2}\left(\ln\frac{\Omega}{2T_c}\ \tanh\left[\frac{\Omega}{2T_c}\right] - \int_{E=0}^{\Omega}\frac{\ln E}{\cosh^2\left[E/2T_c\right]}\right) \equiv f(\kappa)R(T_c,\Omega,\mu). \quad (18)$$

Equation (18) gives for critical temperature

$$T_c = 1.14\Omega\exp\left[-\frac{1}{\lambda f(\kappa)}\right]. \quad (19)$$

Figure 5 demonstrates that the critical temperature has a sharp spike at the transition point $w = v$. The ratio $\frac{2\Delta}{T_c}$ is still universal for any w/v.

To summarize, superconductivity in Weyl semimetal with tilted Dirac cones that in the normal phase undergoes a topological ("2.5") transition from type-I to type-II semimetal was theoretically considered. We calculated in the framework of the phonon-mediated pairing model the spectrum of the superconducting quasiparticles, spectral density, critical temperature, and the superconducting gap as the function of the tilt parameter w/v. The critical temperature and the superconducting energy gap of Weyl semimetal have spikes at the transition point $w/v = 1$. The quasiparticle spectrum in the superconducting state qualitatively discriminates between type I and type II; see Fig. 2. In particular, the sharp cone pinnacle in the excitations spectrum wedge typical for a type I disappears, and two parallel nearly flat bands are formed. The spectral density $A(\mathbf{p},E)$ is also undergoing modification under type-I-to-type-II topological phase transition; see Fig. 3.

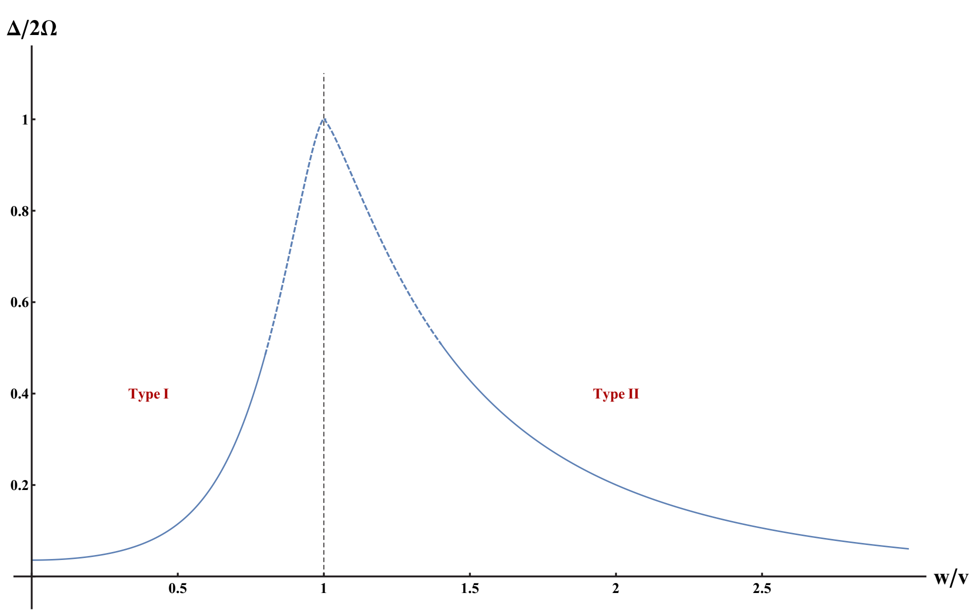

FIG. 5. The superconducting gap at zero temperature versus cone tilted parameter κ. (The dashed line marks the region beyond assumption $\mu \gg \Omega \gg T_c$.) Cutoff parameter: $\delta = 0.01$, $\mu = 3$, $\lambda = 0.15$.

V. DISCUSSION AND CONCLUSIONS

We discuss next an application of the results to recent measurements on the superconductivity of a compound that has Weyl semimetal signatures under pressure. In particular, in intercalated $Sr_{0.065}Bi_2Se_3$ single crystal superconductivity first is suppressed, but at a high pressure of 6 GPa it reappears and reaches a relatively high T_c of 10 K that persists up to 80 GPa. The increase is not gradual, but rather abrupt in the region of 15 GPa. It was discovered recently that, while parameters of the system (the electron-phonon coupling, Debye frequency Ω) between two structural phase transitions smoothly depend on a pressure, the tilt parameter is very sensitive to stress [15,21]. Our result might provide an explanation of a spike in dependence of T_c on pressure in single crystals observed in many superconducting semimetals [26–28].

The experimental situation is not unambiguous. There are structural phase transitions that might cause an abrupt change of electron-phonon coupling. Efforts have been made to associate the changes of T_c with such transitions. For example, in [27] such a maximum in T_c takes place close to the structural phase transition from $C2/m$ (sevenfold) to phase $C2/m$ (bcc). On the other hand, results presented in [28] *are clearly separated from structural phase transitions, giving evidence that this maximum is caused by undergoing type-I-to-type-II topological transition in semimetals*.

The problem of the applicability of the BCS approach and a related issue of Migdal's theorem, i.e., the adiabatic limit ($\mu \gg \Omega$) in Weyl semimetals, has been addressed in detail by DasSarma's group and in our earlier paper [32]. The energy gap in this systems does not exceed 10 K, while Ω is 100 K and chemical potential in the thousands, as in conventional optical phonon BCS. This justifies our BCS approach.

Although a very specific simple model of a two-dimensional single pair of Dirac cones was employed, it is expected that generalization to similar physical systems like the surfaces of 3D topological insulators and 3D Weyl semimetals will lead to similar conclusions.

ACKNOWLEDGMENTS

We are grateful to T. Maniv, T. W. Luo, M. Lewkowicz, C. C. Hou, and E. Farber for valuable discussions. B.R. was supported by NSC of R.O.C. Grant No. 103-2112-M-009-014-MY3 and the MOE ATU program. The work of D.L. also is supported by National Natural Science Foundation of China (Grants No. 11274018 and No. 11674007). B.R. is grateful to School of Physics of Peking University and Bar Ilan Center for Superconductivity for hospitality.

APPENDIX A: GORKOV EQUATIONS FOR A TWO-SUBLATTICE SYSTEM

In this appendix Gorkov equations for a two-sublattice system (index $\alpha = 1,2$) in Matsubara representation $t = -i\tau$ are briefly derived.

The equation of motion for creation and annihilation Matsubara operators reads ($\hbar = 1$)

$$\frac{\partial \psi_\gamma^+}{\partial \tau} = [H,\psi_\gamma^+]; \quad \frac{\partial \psi_\gamma}{\partial \tau} = [H,\psi_\gamma]. \tag{A1}$$

The Matsubara Green's function is defined as

$$G_{\alpha\beta}^{ts}(X,X') = \delta^{ts} g_{\alpha\beta}(X,X') = -\langle T_\tau \{\psi_\alpha^t(X)\psi_\beta^{s+}(X')\}\rangle, \tag{A2}$$

$$F_{\alpha\beta}^{ts}(X,X') = -\varepsilon^{ts} f_{\alpha\beta}(X,X') = \langle T_\tau \{\psi_\alpha^t(X)\psi_\beta^s(X')\}\rangle,$$
$$F_{\alpha\beta}^{+ts}(X,X') = \varepsilon^{ts} f_{\alpha\beta}^+(X,X') = \langle T_\tau \{\psi_\alpha^{t+}(X)\psi_\beta^{s+}(X')\}\rangle, \tag{A3}$$

where X combines space and time and T_τ is the imaginary time-ordered product [36]. The time derivatives using the equations of motion are written via the following commutators:

$$\frac{\partial G_{\gamma\kappa}^{st}(X,X')}{\partial \tau} = -\langle T_\tau\{[H,\psi_\gamma^s(X)]\psi_\kappa^{t+}(X')\}\rangle - \delta^{\gamma\kappa}\delta^{ts}\delta(X-X'),$$
$$\frac{\partial F_{\gamma\kappa}^{st+}(X,X')}{\partial \tau} = \langle T_\tau\{[H,\psi_\gamma^{s+}(X)]\psi_\kappa^{t+}(X')\}\rangle.$$

This leads to

$$\frac{\partial G_{\gamma\kappa}^{st}(X,X')}{\partial \tau} = -\left\langle T_\tau \begin{Bmatrix} -\int_{r''}\{iv\sigma_{\gamma\beta}^i\delta_{r_i''}'(r-r'') - \mu'\delta_{\gamma\beta}\delta(r-r'')\}\psi_\beta^s(X'')\psi_\kappa^{t+}(X') \\ +\frac{g^2}{4}\varepsilon^{s_1 s}\varepsilon^{s_3 s_2}\psi_\alpha^{\dagger s_1}(X)\psi_\alpha^{s_3}(X)\psi_\gamma^{s_2}(X)\psi_\kappa^{t+}(X') \end{Bmatrix}\right\rangle - \delta^{\gamma\kappa}\delta^{ts}\delta(X-X'), \tag{A4}$$

$$\frac{\partial F_{\gamma\kappa}^{st+}(X,X')}{\partial \tau} = \left\langle T_\tau \begin{Bmatrix} \int_{r''}\{-iv\nabla_{r''}^i\delta(r''-r)\sigma_{\alpha\gamma}^i - \mu'\delta(r''-r)\delta_{\alpha\gamma}\}\psi_\alpha^{+s}(r'')\psi_\kappa^{t+}(X') \\ +\frac{g^2}{4}\varepsilon^{s_1 s_2}\varepsilon^{s_3 s}\psi_\alpha^{\dagger s_1}(\mathbf{r})\psi_\gamma^{+s_2}(\mathbf{r})\psi_\alpha^{s_3}(\mathbf{r})\psi_\kappa^{t+}(X') \end{Bmatrix}\right\rangle. \tag{A5}$$

Here $\mu' = \mu - wp_x$.

The correlators are calculated within the Gaussian approximation below:

For the same X, $F_{\alpha\beta}^* = -\langle T_\tau \psi_\beta^+\psi_\alpha^+\rangle \to F_{\alpha\beta}^+ = F_{\beta\alpha}^*$. Using spin symmetry one obtains in Gaussian approximation $\Delta_{\alpha\gamma} = -\frac{g^2}{4}\varepsilon^{s_3 s_2}\langle\psi_\alpha^{s_3}(X)\psi_\gamma^{s_2}(X)\rangle$. Thus, one obtains the first Gorkov equation:

$$-\frac{\partial}{\partial \tau} g_{\gamma\kappa}(X,X') - iv\sigma_{\gamma\beta}^i \nabla_r^i g_{\beta\kappa}(X,X') + \mu' g_{\beta\kappa}(X,X') + \Delta_{\alpha\gamma} f_{\alpha\kappa}^+(X,X') = \delta^{\gamma\kappa}\delta(X-X'). \tag{A6}$$

Similarly, the second equation takes the form

$$\frac{\partial}{\partial\tau} f^{+}_{\gamma\kappa}(X,X') - iv\sigma^{i}_{\alpha\gamma}\nabla^{i}_{r} f^{+}_{\alpha\kappa}(X,X') + \mu' f^{+}_{\gamma\kappa}(X,X') - \Delta^{*}_{\alpha\gamma} g_{\alpha\kappa}(X,X') = 0. \quad \text{(A7)}$$

For a uniform system, using the Fourier transform, $g_{\gamma\kappa}(X) = T\sum_{\omega p}\exp[i(-\omega\tau + pr)]g_{\gamma\kappa}(\omega,p)$, with Matsubara frequencies, $\omega_n = 2\pi T(n+1/2)$, one obtains

$$\left[vp^{i}\sigma^{i}_{\gamma\beta} + (i\omega + \mu - wp_x)\delta_{\gamma\beta}\right]g_{\beta\kappa}(\omega,p) + \Delta_{\alpha\gamma} f^{+}_{\alpha\kappa}(\omega,p) = \delta^{\gamma\kappa}, \quad \text{(A8)}$$

$$\left[vp^{i}\sigma^{i}_{\beta\gamma} + (-i\omega + \mu - wp_x)\delta_{\gamma\beta}\right]f^{+}_{\beta\kappa}(\omega,p) - \Delta^{*}_{\alpha\gamma} g_{\alpha\kappa}(\omega,p) = 0. \quad \text{(A9)}$$

The singlet ansatz

$$\Delta_{\alpha\gamma} = \sigma^{x}_{\alpha\gamma}\Delta \quad \text{(A10)}$$

simplifies the equations

$$\left[vp^{i}\sigma^{i}_{\gamma\beta} + (i\omega + \mu - wp_x)\delta_{\gamma\beta}\right]g_{\beta\kappa}(\omega,p) + \Delta\sigma^{x}_{\alpha\gamma} f^{+}_{\alpha\kappa}(\omega,p) = \delta^{\gamma\kappa}, \quad \text{(A11)}$$

$$\left[vp^{i}\sigma^{i}_{\beta\gamma} + (-i\omega + \mu - wp_x)\delta_{\gamma\beta}\right]f^{+}_{\beta\kappa}(\omega,p) - \Delta^{*}\sigma^{x}_{\gamma\alpha} g_{\alpha\kappa}(\omega,p) = 0. \quad \text{(A12)}$$

Casting this in the matrix form,

$$(vp^{i}\sigma^{i} + i\omega + \mu - wp_x)\widehat{g} + \Delta\sigma^{x}\widehat{f}^{+} = I, \quad \text{(A13)}$$

$$(vp^{i}\sigma^{ti} - i\omega + \mu - wp_x)\widehat{f}^{+} - \Delta^{*}\sigma^{x}\widehat{g} = 0, \quad \text{(A14)}$$

it is easily solved. Substituting g from the second equation,

$$\sigma^{x}[vp^{i}\sigma^{ti} + (-i\omega + \mu - wp_x)I]\widehat{f}^{+} = \Delta^{*}\widehat{g}, \quad \text{(A15)}$$

one explicitly obtains the anomalous correlator

$$\widehat{f}^{+} = M^{-1}\Delta^{*}, \quad \text{(A16)}$$

where

$$M = (vp^{i}\sigma^{i} + i\omega + \mu - wp_x) \times \sigma^{x}[v\sigma^{tj}p^{j} + (-i\omega + \mu - wp_x)] + \Delta\Delta^{*}\sigma^{x}. \quad \text{(A17)}$$

The correlator determining the excitation spectrum consequently is

$$\widehat{g} = \sigma^{x}[p^{i}\sigma^{ti} + (-i\omega + \mu - wp_x)I]M^{-1}\Delta^{*}.$$

The dispersion relations in the text are defined by zeros of the determinant,

$$\det[M] = -[\Delta^2 + (vp - \mu + wp_x)^2 + \omega^2] \times [\Delta^2 + (vp + \mu - wp_x)^2 + \omega^2]. \quad \text{(A18)}$$

In this section, the details of the calculation of the superconducting gap at zero temperature and of the critical temperature are given.

APPENDIX B: ZERO-TEMPERATURE GAP

At zero temperature the gap is determined by the self-consistency equation:

$$\Delta^{*} = \frac{\Delta^{*}}{2(2\pi)^3}\int d\omega d\mathbf{p}\,\mathrm{Tr}\,[\sigma_x M^{-1}]. \quad \text{(B1)}$$

At zero temperature the summation over Matsubara frequencies was replaced by integration. The resulting integral,

$$\frac{1}{g^2} = \frac{1}{(2\pi)^3}\int d\omega d\mathbf{p}\frac{v^2p^2 + \Delta^2 + (\mu - wp_x)^2 + \omega^2}{[\Delta^2 + (vp + wp_x - \mu)^2 + \omega^2][\Delta^2 + (vp - wp_x + \mu)^2 + \omega^2]}, \quad \text{(B2)}$$

is first performed over ω:

$$\frac{1}{g^2} = \frac{1}{4(2\pi)^2}\int_{\theta=0}^{2\pi} d\theta \int pdp \left\{ \begin{array}{l} \frac{1}{[\Delta^2+(\varepsilon-\mu)^2]^{1/2}} + \frac{1}{[\Delta^2+(2wp_x+\varepsilon+\mu)^2]^{1/2}} \\ -\frac{1}{[\Delta^2+(\varepsilon-\mu)^2]^{1/2}+[\Delta^2+(2wp_x+\varepsilon+\mu)^2]^{1/2}} \end{array} \right\}. \quad \text{(B3)}$$

The resulting expression is already given in polar coordinates and, in addition, the energy as function of the polar angle,

$$\varepsilon(p,\theta) = vp + wp_x = vp(1 + \kappa\cos\theta), \quad \text{(B4)}$$

was used. Here $\kappa = \frac{w}{v}$.

In the adiabatic (BCS) limit, when $\mu \gg \Omega \gg \Delta$, the integration is limited to the shell shown in Fig. 4 in both phases. Changing the integration variable to ε, one obtains

$$\frac{1}{g^2} = \frac{1}{4(2\pi)^2v^2}\int_0^{2\pi} d\theta\frac{\mathrm{sgn}(1+\kappa\cos\theta)}{(1+\kappa\cos\theta)^2} \times \int_{\varepsilon=-\Omega}^{\Omega}(\varepsilon+\mu)\frac{d\varepsilon}{(\Delta^2+\varepsilon^2)^{1/2}} \quad \text{(B5)}$$

$$= \frac{\mu}{4(2\pi)v^2}f(\kappa)\int_{\varepsilon=-\Omega}^{\Omega}\frac{d\varepsilon}{(\Delta^2+\varepsilon^2)^{1/2}} \quad \text{(B6)}$$

$$= \frac{\mu}{4\pi v^2}f(\kappa)\ln\left[\frac{\Omega + \sqrt{\Delta^2+\Omega^2}}{\Delta}\right]. \quad \text{(B7)}$$

Here the integration over azimuthal angle θ was obtained by replacing variables θ with $x = v/w + \cos\theta$. In the case $w/v < 1$ (type-I semimetal phase), $x > 0$ and the integral over the azimuthal angle reads

$$f(\kappa) = \frac{1}{\pi}\int_{\theta}\frac{1}{(1+\kappa\cos\theta)^2} = \frac{2}{(1-\kappa^2)^{3/2}}. \quad \text{(B8)}$$

In the case $w > v$ (type-II semimetal phase) the integral might be modified as

$$f\left(\frac{w}{v}\right) = -\frac{1}{\pi}\int_{x=v/w+1}^{v/w-1} dx \frac{\mathrm{sgn}(x)}{\sqrt{1-(x-v/w)^2 x^2}} \tag{B9}$$

$$= \frac{1}{\pi}\int_{x=v/w-1}^{0} \frac{dx}{\sqrt{1-(x-v/w)^2 x^2}} - \frac{1}{\pi}\int_{0}^{v/w+1} \frac{dx}{\sqrt{1-(x-v/w)^2 x^2}}. \tag{B10}$$

Equation (B9) represented in equivalent form

$$\lim_{\delta\to 0}\frac{1}{\pi}\int_{x=\delta}^{-v/w+1} \frac{dx}{x^2}\left[\frac{1}{\sqrt{1-(x+1/w)^2}} - \frac{1}{\sqrt{1-(x-1/w)^2}}\right]$$
$$-\frac{1}{\pi}\int_{-v/w+1}^{v/w+1} \frac{dx}{\sqrt{1-(x-v/w)^2 x^2}}, \tag{B11}$$

and performing the integration in (B11), we obtain

$$f(\kappa) = \frac{2\kappa^2}{\pi(\kappa^2-1)^{3/2}}\left\{2\sqrt{1+\kappa} - 1 + \ln\frac{2(\kappa^2-1)}{\kappa(1+\sqrt{1+\kappa})^2\delta}\right\}, \tag{B12}$$

from which the Eq. (18) of the paper follows. Here $\delta = \pi a\Omega/w\hbar$ is the cutoff parameter.

APPENDIX C: CRITICAL TEMPERATURE

The critical temperature is defined from the second Gorkov equation with vanishing Δ:

$$\frac{1}{g^2} = \frac{T}{(2\pi)^2}\int d\mathbf{p}\sum\nolimits_n \frac{v^2p^2 + (\mu - wp_x)^2 + \omega_n^2}{\left[(vp + wp_x - \mu)^2 + \omega_n^2\right]\left[(vp - wp_x + \mu)^2 + \omega_n^2\right]}. \tag{C1}$$

Performing summation over ω_n, one obtains

$$\frac{1}{g^2} = \frac{1}{4(2\pi)^2}\int_{\theta=0}^{2\pi}\int pdp\left\{\frac{\tanh\left[\frac{|p(v+w\cos\theta)-\mu|}{2T}\right]}{|p(v+w\cos\theta)-\mu|} + \frac{\tanh\left[\frac{|p(v+w\cos\theta)+\mu|}{2T}\right]}{|p(v+w\cos\theta)+\mu|}\right\}. \tag{C2}$$

In the adiabatic approximation, $\mu \gg \Omega$, we get, as in the previous case,

$$\frac{1}{g^2} = \frac{\mu}{8\pi v^2} f(\kappa)\left\{2\left(\ln\frac{\Omega}{2T_c}\ \tanh\left[\frac{\Omega}{2T_c}\right] - \int_{\varepsilon=0}^{\Omega} d\varepsilon\frac{\ln\varepsilon}{\cosh^2\left[\frac{\varepsilon}{2T_c}\right]}\right) + \frac{\Omega}{\mu}\right\}. \tag{C3}$$

In this limit Eq. (C3) reads for critical temperature

$$T_c = \frac{\pi}{4\gamma_E}\Omega\exp\left[-\frac{4\pi v^2}{\mu g^2 f(\kappa)}\right], \tag{C4}$$

where $\ln[\gamma_E] = 0.577$.

[1] I. M. Lifshitz, M. Ya. Azbel, and M. I. Kaganov, *Electron Theory of Metals* (Springer, New York, 2012).

[2] I. M. Lifshitz, Zh. Eksp. Teor. Fiz. **38**, 1569 (1960) [Sov. Phys. JETP **11**, 1130 (1960)].

[3] Ya. M. Blanter, M. I. Kaganov, A. V. Pantsulaya, and A. A. Varlamov, Phys. Rep. **245**, 159 (1994).

[4] C. N. Louis and K. Iyakutti, Phys. Rev. B **67**, 094509 (2003).

[5] G. E. Volovik, arXiv:1604.00849v5; Y. Xu, F. Zhang, and C. Zhang, Phys. Rev. Lett. **115**, 265304 (2015).

[6] K. Novoselov, A. K. Geim, S. Morozov, D. Jiang, M. Katsnelson, I. Grigorieva, S. Dubonos, and A. Firsov, Nature (London) **438**, 197 (2005); M. I. Katsnelson, *Graphene. Carbon in Two Dimensions* (Cambridge University Press, Cambridge, UK, 2012).

[7] B. Feng, Jin Zhang, Qing Zhong, W. Li, S. Li, H. Li, P. Cheng, S. Meng, L. Chen, and K. Wu, Nat. Chem. **8**, 563 (2016); M. E. Dvila, L. Xian, S. Cahangirov, A. Rubio, and G. Le Lay, New J. Phys. **16**, 095002 (2014); P.-H. Shih, Y.-H. Chiu, J.-Y. Wu, F.-L. Shyu, and M.-F. Lin, Sci. Rep. **7**, 40600 (2017).

[8] M. Neupane, S.-Y. Xu, R. Sankar *et al.*, Nat. Commun. **5**, 3786 (2014); Z. K. Liu *et al.*, Nat. Mater. **13**, 677 (2014).

[9] Z. Wang, X.-F. Zhou, X. Zhang, Q. Zhu, H. Dong, M. Zhao, and A. R. Oganov, Nano Lett. **15**, 6182 (2015); L. He,

Y. Jia, S. Zhang, X. Hong, C. Jin, and S. Li, Quantum Mater. **1**, 16014 (2016).

[10] J. Singleton and C. Mielke, Contemp. Phys. **43**, 63 (2002); N. Tajima, S. Sugawara, R. Kato, Y. Nishio, and K. Kajita, Phys. Rev. Lett. **102**, 176403 (2009); K. Kajita, Y. Nishio, N. Tajima, Y. Suzumura, and A. Kobayashi, J. Phys. Soc. Jpn. **83**, 072002 (2014).

[11] S. Katayama, A. Kobayashi, and Y. Suzumura, J. Phys. Soc. Jpn. **75**, 054705 (2006); M. O. Goerbig, J.-N. Fuchs, G. Montambaux, and F. Piéchon, Phys. Rev. B **78**, 045415 (2008); M. Hirata *et al.*, Nat. Commun. **7**, 12666 (2016).

[12] M. Monteverde, M. O. Goerbig, P. Auban-Senzier, F. Navarin, H. Henck, C. R. Pasquier, C. Mèziére, and P. Batail, Phys. Rev B **87**, 245110 (2013).

[13] H. Zhang, C.-X. Liu, X.-L. Qi, X. Dai, Z. Fang, and S.-C. Zhang, Nat. Phys. **5**, 438 (2009); Y. Xia, D. Qian, D. Hsieh, L. Wray, A. Pal, H. Lin, A. Bansil, D. Grauer, Y. S. Hor, R. J. Cava, and M. Z. Hasan, *ibid.* **5**, 398 (2009).

[14] A. A. Soluyanov, D. Gresch, Z. Wang, Q. Wu, M. Troyer, X. Dai, and B. A. Bernevig, Nature (London) **527**, 495 (2015).

[15] J. Ruan, S.-K. Jian, H. Yao, H. Zhang, S.-C. Zhang, and D. Xing, Nat. Commun. **7**, 11136 (2016).

[16] Y. Sun, S.-C. Wu, M. N. Ali, C. Felser, and B. Yan, Phys. Rev. B **92**, 161107(R) (2015); L. Huang, T. M. McCormick, M. Ochi, Z. Zhao, M.-T. Suzuki, R. Arita, Y. Wu, D. Mou, H. Cao, J. Yan, N. Trivedi, and A. Kaminski, Nat. Mater. **15**, 1155 (2016); Y. Wang *et al.*, Nat. Commun. **7**, 13142 (2016); K. Deng *et al.*, Nat. Phys. **12**, 1105 (2016); J. Jiang, Z. K. Liu, Y. Sun, H. F. Yang, C. R. Rajamathi, Y. P. Qi, L. X. Yang, C. Chen, H. Peng, C.-C. Hwang, S. Z. Sun, S.-K. Mo, I. Vobornik, J. Fujii, S. S. P. Parkin, C. Felser, B. H. Yan, and Y. L. Chen, Nat. Commun. **8**, 13973 (2017).

[17] Mingzhe Yan *et al.*, arXiv:1607.03643v1.

[18] I. Belopolski *et al.*, Nat. Commun. **7**, 13643 (2016).

[19] G. Chang *et al.*, arXiv:1604.02124.

[20] F. Sun and J. Ye, arXiv:1610.03171v1.

[21] Y. Zhou, P. Lu, Y. Du, X. Zhu, G. Zhang, R. Zhang, D. Shao, X. Chen, X. Wang, M. Tian, J. Sun, X. Wan, Z. Yang, W. Yang, Y. Zhang, and D. Xing, Phys. Rev. Lett. **117**, 146402 (2016).

[22] Y. S. Hor, A. J. Williams, J. G. Checkelsky, P. Roushan, J. Seo, Q. Xu, H. W. Zandbergen, A. Yazdani, N. P. Ong, and R. J. Cava, Phys. Rev. Lett. **104**, 057001 (2010); H. Yi *et al.*, Sci. Rep. **4**, 6106 (2014).

[23] S. Wanka, D. Beckmann, and J. Wosnitza, E. Balthes and D. Schweitzer, W. Strunz, and H. J. Keller, Phys. Rev. B **53**, 9301 (1996).

[24] Edited by V. Z. Kresin and W. A. Little, *Organic Superconductivity* (Springer Science+Business Media, New York, 1990); V. Vulcanescu, C. Lenoir, P. Batail, and L. Fruchter, Phys. Rev. B **52**, 471 (1995); K. Izawa, H. Yamaguchi, T. Sasaki, and Y. Matsuda, Phys. Rev. Lett. **88**, 027002 (2001); S. Milbradt, A. A. Bardin, C. J. S. Truncik, W. A. Huttema, A. C. Jacko, P. L. Burn, S. C. Lo, B. J. Powell, and D. M. Broun, Phys. Rev. B **88**, 064501 (2013); H. B. Cui, H. Kobayashi, S. Ishibashi, M. Sasa, F. Iwase, R. Kato, and A. Kobayashi, J. Am. Chem. Soc. **136**, 7619 (2014).

[25] Y. Qi *et al.*, Nat. Commun. **7**, 11038 (2016).

[26] Y. Zhou, X. Chen, R. Zhang, J. Shao, X. Wang, C. An, Y. Zhou, C. Park, W. Tong, L. Pi, Z. Yang, C. Zhang, and Y. Zhang, Phys. Rev. B **93**, 144514 (2016).

[27] J. J. Hamlin, J. R. Jeffries, N. P. Butch, P. Syers, D. A. Zocco, S. T. Weir, Y. K. Vohra, J. Paglione, and M. B. Maple, J. Phys.: Condens. Matter **24**, 035602 (2012); K. Kirshenbaum, P. S. Syers, A. P. Hope, N. P. Butch, J. R. Jeffries, S. T. Weir, J. J. Hamlin, M. B. Maple, Y. K. Vohra, and J. Paglione, Phys. Rev. Lett. **111**, 087001 (2013).

[28] P. P. Kong *et al.*, J. Phys.: Condens. Matter **25**, 362204 (2013).

[29] R. L. Stillwell, Z. Jenei, S. T. Weir, Y. K. Vohra, and J. R. Jeffries, Phys. Rev. B **93**, 094511 (2016); D. VanGennep *et al.*, J. Phys.: Condens. Matter **29**, 09LT02 (2017).

[30] Y. Qi, W. Shi, P. G. Naumov, N. Kumar, W. Schnelle, O. Barkalov, C. Shekhar, H. Borrmann, C. Felser, B. Yan, and S. A. Medvedev, Phys. Rev. B **94**, 054517 (2016).

[31] P. L. Alireza *et al.*, arXiv:1610.09790v1.

[32] S. Das Sarma and Q. Li, Phys. Rev. B **88**, 081404(R) (2013); P. M. R. Brydon, S. Das Sarma, H.-Y. Hui, and J. D. Sau, *ibid.* **90**, 184512 (2014); D. P. Li, B. Rosenstein, B. Ya. Shapiro, and I. Shapiro, *ibid.* **90**, 054517 (2014).

[33] L. Fu and E. Berg, Phys. Rev. Lett. **105**, 097001 (2010).

[34] J.-L. Zhang *et al.*, Front. Phys. **7**, 193 (2012).

[35] M. Alidoust, K. Halterman, and A. A. Zyuzin, arXiv:1612.05003v1.

[36] A. A. Abrikosov, L. P. Gor'kov, and I. E. Dzyaloshinskii, *Quantum Field Theoretical Methods in Statistical Physics* (Pergamon, New York, 1965).